70-14,846

PARKER, Gerhard Hans, 1943-
TUNNELING IN SCHOTTKY BARRIERS.

California Institute of Technology, Ph.D., 1970
Physics, electronics and electricity

University Microfilms, A XEROX Company, Ann Arbor, Michigan

THIS DISSERTATION HAS BEEN MICROFILMED EXACTLY AS RECEIVED

TUNNELING IN SCHOTTKY BARRIERS

Thesis by

Gerhard H. Parker

In Partial Fulfillment of the Requirements

For the Degree of

Doctor of Philosophy

California Institute of Technology

Pasadena, California

1970

(Submitted October 31, 1969)

Acknowledgments

The author wishes to express his appreciation to Dr. Carver A. Mead for his guidance and encouragement. The unique nature of InAs was pointed out to the author by F. A. Padovani of Texas Instruments and the CdTe was supplied by L. van Atta, G. Picus and N. Kyle of the Hughes Research Laboratories. The work was supported in part by the Office of Naval Research. The author also gratefully acknowledges financial support received from the National Science Foundation and Fairchild Semiconductor Corporation.

Abstract

The tunneling characteristics of metal contacts on n-type CdTe and p-type InAs have been measured. Both the forward and reverse bias characteristics on CdTe are in good agreement with the two-band model for the energy vs. complex momentum relationship. The presence of trapping states increased the magnitude of the tunneling current at low voltage levels by providing a two-step transition. The slope of the forward bias log J vs. V curves for tunneling through the intermediate states was reduced by a factor of 2 . The approximate density and energy of the trapping states was calculated from the observed J-V characteristics. The E-k dispersion relation for InAs was also determined and found to be in excellent agreement with the two-band model.

Table of Contents

Chapter I

Introduction

A metal-semiconductor (Schottky barrier) is the rectifying junction formed by the intimate contact of a metal and a semiconductor having nonequal work functions or electronegativities.[1] The device is dominated by majority carrier current flow, that is, electrons for n-type and holes for p-type semiconductors. The current flow mechanism can be by either thermionic or field emission. The thermionic emission models postulated by Mott[2] and Schottky[3] were successful in explaining the behavior of early metal semiconductor junctions. Later, in 1942, Bethe[4] showed drastic departures from the currents predicted by the thermionic emission models in barriers made on heavily doped silicon. He attributed this discrepancy to tunneling through the barrier.

Interest in a quantitative description of tunneling was rekindled in 1965 when Lewicki and co-workers[5,6,7] showed that it was possible to determine energy dependence of the imaginary part of the electron wave vector in the forbidden gap of an insulator or semiconductor by measurements of tunneling current as a function of thickness and applied voltage. Later in an elegant series of experiments Padovani and Stratton[8] applied a similar technique to Schottky barriers on GaAs, a material which has subsequently been studied by other workers.[9,10] Since both the thickness of the depletion layer and the energy of the final state depend upon applied voltage, they were able to characterize a considerable portion of the energy gap with a simple voltage-current measurement on a single sample.

The study of other materials has been restricted somewhat by the problems of obtaining the high carrier concentrations necessary for the formation of narrow space charge regions with the Schottky barriers. The present work deals in part with tunneling through barriers on n-type CdTe in the carrier concentration range 1.3×10^{17} to 6.0×10^{17} cm^{-3}, as compared to the 10^{18} or 10^{19} cm^{-3} used in the GaAs experiments. The low concentration reduces the magnitude of the forward bias tunneling current to a point where it is possible to observe tunneling through the forbidden gap only near the band edge. The results are nonetheless useful in that they give a measure of the E-k dispersion relation near the band edge and hence a measure of the effective mass of the light electron or hole bands. Information about the E-k relation near mid-gap was obtained by measuring the reverse bias tunneling characteristics as a function of barrier energy. The results of tunneling experiments on CdTe also indicate that the presence of trapping centers can play an important role in the tunneling process.

A second semiconductor, InAs, was selected because the barrier energy on p-type material is nearly equal to the band gap, thereby making the entire forbidden gap accessible. InAs has the further advantage of having a narrow band gap and low effective mass charge carriers, both of which are favorable for high tunneling current densities. Thus, it was possible to experimentally determine the E-k dispersion relation through almost the entire forbidden gap from the tunneling J-V characteristics of Schottky barriers.

Some of the work reported here has been published under the following titles:

"Energy-Momentum Relationship in InAs," G. H. Parker and C. A. Mead, Phys. Rev. Letters 21, 605 (1968).

"The Effect of Trapping States on Tunneling in Metal-Semiconductor Junctions," G. H. Parker and C. A. Mead, Appl. Phys. Letters 14, 21 (1969).

"Tunneling in CdTe Schottky Barriers," G. H. Parker and C. A. Mead, Phys. Rev. 184, 780 (1969).

Chapter II

Theory

We shall first restrict ourselves to the low temperature J-V characteristics of thin Schottky barriers, i.e. where the primary current mechanism is the quantum mechanical tunneling of electrons through the barrier. When the diode is under forward bias at low temperatures, the tunneling occurs from the edge of the space charge region at the conduction band energy through the barrier into the metal. Under reverse bias tunneling occurs from the metal to the conduction band in the semiconductor. These two cases will be treated separately since in the forward bias case both the region of the forbidden gap through which tunneling takes place and the tunneling distance are functions of voltage whereas in the reverse bias case only the latter varies.

II.1 Forward J-V Characteristics

As seen in Fig. 1 the potential energy, E, of the barrier as measured with respect to the energy at the bottom of the conduction band in the bulk of the material is given by[11]

$$E = Nq(\ell-x)^2/2\epsilon \qquad (1)$$

where N is the impurity concentration in the semiconductor, q is the charge on the electron, x is the distance measured from the metal, ϵ is the permittivity of the semiconductor and

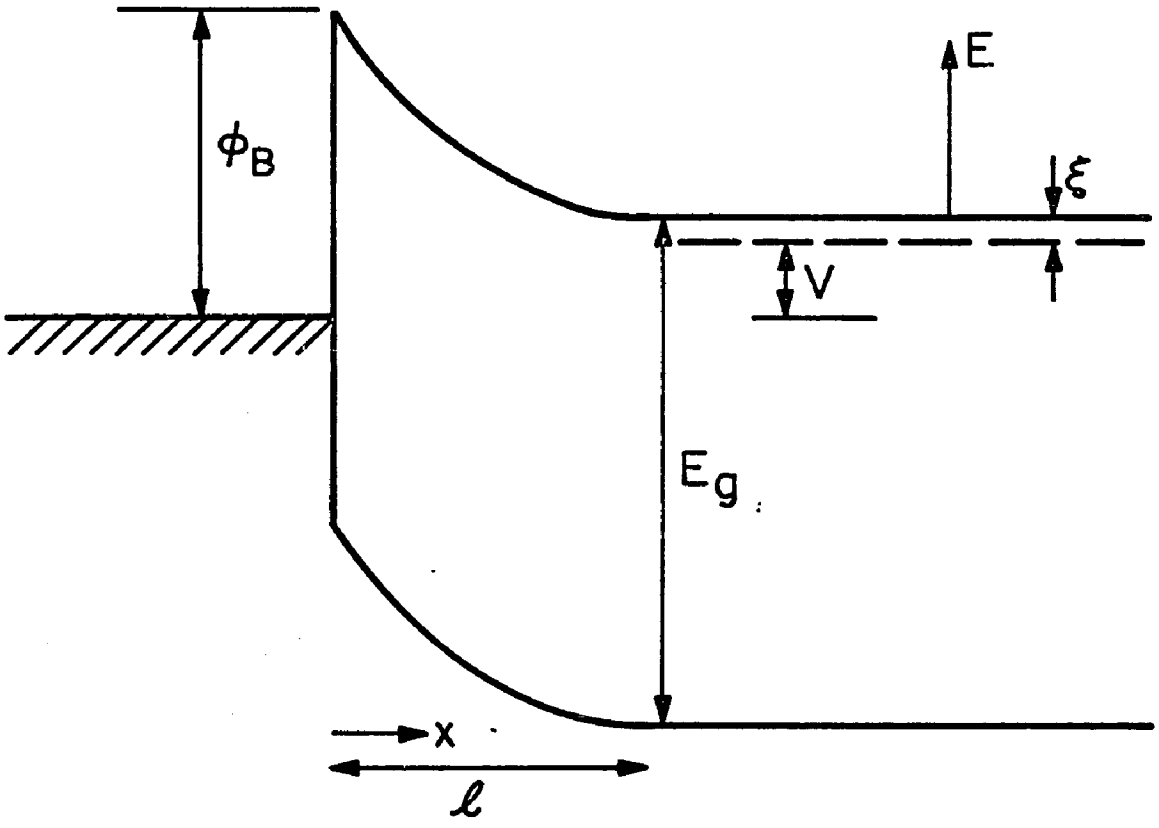

Fig. 1. Electron potential energy diagram of a Schottky barrier.

$$\ell = \left[2\varepsilon(\phi_B - V + \xi)/Nq\right]^{\frac{1}{2}} \tag{2}$$

is the width of the space charge layer in the semiconductor. Here ϕ_B is the barrier energy and ξ is the semiconductor Fermi energy from the conduction band edge, both given in electron volts.

In order to calculate the tunneling current, we must assume a specific energy-momentum relationship for the electrons in the forbidden gap. The solution to Schrödinger's equation for the motion of electrons in a periodic potential using the "nearly free electron" approximation results in the following expression[12]

$$E = \tfrac{1}{2}E_g \pm \tfrac{1}{2}\sqrt{E_g^2 - \frac{2\hbar^2 k^2 E_g}{m^*}} \tag{3}$$

where E is the energy measured from the conduction band minimum, E_g is the band gap of the semiconductor, $\hbar$ is Planck's constant, and m^* the effective mass of the electron. k is the wave vector which is real in the conduction and valence bands, zero at the band edges, and imaginary in the forbidden gap, as shown in Fig. 2. This idealized solution requires equal values for the effective mass of the charge carriers in the conduction and valence bands. In many low band gap semiconductors, the effective masses of the light conduction and valence bands are nearly equal and this solution in fact does represent a realistic approximation.[10,13] For small values of k, i. e. near the conduction band, Eq. 3 reduces to

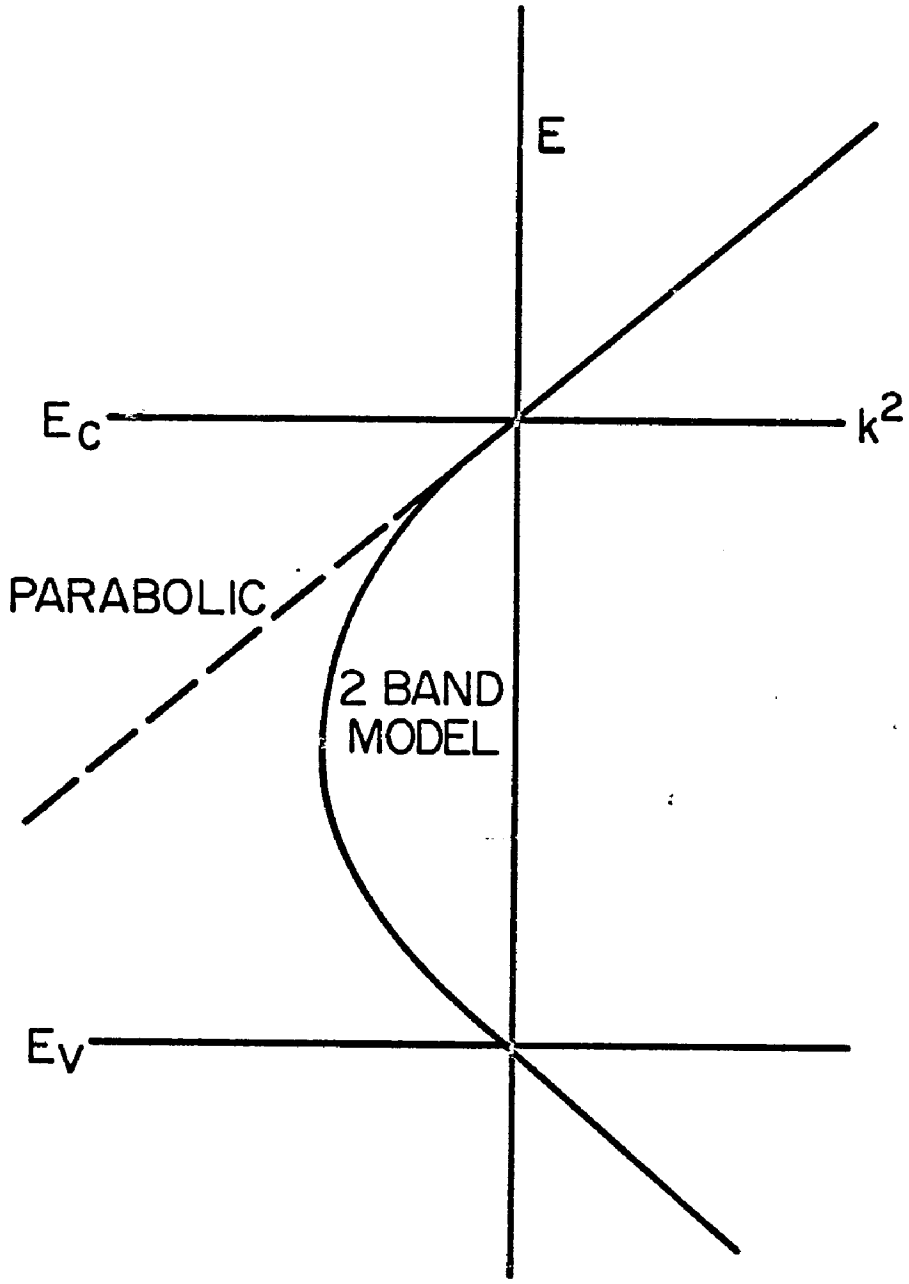

Fig. 2. Electron energy, E , versus wave vector, k .

$$E = \frac{\hbar^2 k^2}{2m^*} \tag{4}$$

The expression presented in Eq. 3 is commonly referred to as the two-band model and the expression in Eq. 4 the parabolic model. Figure 2 illustrates the E-k relationship described by the two equations.

We can now proceed to calculate the form of the tunneling current. For forward bias voltage greater than a few kT/q , the electron current is given by :

$$J = J_m e^{-2\int_{\ell}^{o} k dx} \tag{5}$$

where J_m is a slowly varying function of voltage and temperature.[11] In the case of large forward bias, (i. e. when the applied voltage approaches the barrier potential) tunneling occurs through only a small portion of the forbidden gap near the band edge. The parabolic model given by Eq. 4 should be valid in this region. Incorporation of the x dependence of the energy as given in Eq. 1 results in the following expression for the current:

$$J = J_m e^{-s_o(\phi_B - V + \xi)} \tag{6}$$

where

$$s_o = \frac{d \log J}{dV} = \frac{2}{\hbar}\left(\frac{m^* \epsilon}{N}\right)^{\frac{1}{2}}$$

The pre-exponential term, J_m, depends on the width in energy of the electron distribution of the tunneling current. In order to calculate J_m, we must consider the following three cases:

a) $kT/q < 1/s_o < \xi$

The first condition represents a degenerate semiconductor where the energy width of the degeneracy, ξ, is greater than the change in energy, $1/s_o$, necessary to reduce the tunneling probability by $1/e$. Thus, the tunneling takes place from the Fermi energy with a width limited by $1/s_o$. Millea et al.[10] have carried out the detailed calculation for this case. Their result is

$$J_m = \frac{m^* q}{2\pi^2 \hbar^3 C_1^2} \frac{\pi C_1 kT}{\sin(\pi C_1 kT)} \tag{6a}$$

where

$$C_1 = \tfrac{1}{2} s_o q \ell n \left(\frac{4(\phi_B - V)}{\frac{3}{5}\xi} \right)$$

b) $1/s_o > \xi > kT/q$

In the second case the degeneracy energy is smaller than $1/s_o$ and therefore is the limiting energy in the supply function. Based on arguments used to derive Richardson's Constant,[15] the pre-exponential term becomes

$$J_m = \frac{m^* q}{2\pi^2 \hbar^3} (\xi)^2 = A\left(\frac{\xi}{kT}\right)^2 \tag{6b}$$

c) $1/s_o > kT/q$

Finally in the case where the semiconductor is either non degenerate or the degeneracy is less than kT, the supply function is limited by kT and

$$J_m = A = \frac{m^* q}{2\pi^2 \hbar^3} (kT)^2 \tag{6c}$$

For the particular cases to be considered in this work, we encounter all three of these cases and must select the appropriate one depending on the temperature and Fermi energy.[15] The exponential dependence is the same in each case.*

At low forward bias the tunneling will occur through a larger portion of the forbidden gap and some deviation from the parabolic model would be expected. By repeating the calculation using the two-band model we find that

$$J = J_m \exp\left(\frac{2}{3} s_o E_g \left[\left(1 - \frac{\phi_B - V + \xi}{E_g}\right)^{3/2} - 1\right]\right) \tag{7}$$

and

$$\frac{d \log J}{dV} = s = s_o \left(1 - \frac{\phi_B - V + \xi}{E_g}\right)^{\frac{1}{2}}$$

By examining the expression for the slope of the log J vs. V curves, we can see that the correction to the slope derived from the parabolic

---

* For the case of degenerate semiconductors, Conley and Mahan[14] have shown that the ξ in Eq. 6 must be $\frac{3}{5}\xi$.

model is small for large forward bias.

For the general case of an unknown E-k dispersion relation, the current can be expressed as

$$J = J_m \exp\left\{ -\sqrt{\frac{2\epsilon}{qN}} \int_0^{\phi_B - V + \xi} \frac{k}{\sqrt{E}}\, dE \right\} \tag{8}$$

and from there we can go no further. However, given the tunneling J-V characteristics of a Schottky barrier, the energy-momentum dispersion relation can be determined directly. Differentiating Eq. 8 we find

$$\frac{d \log J}{dV} = -\sqrt{\frac{2\epsilon}{Nq}} \frac{k}{\sqrt{\phi_B - V + \xi}} \tag{9}$$

and solving for k^2

$$k^2 = \frac{Nq}{2\epsilon} (\phi_B - V + \xi) \left(\frac{d \log J}{dV}\right)^2 \tag{10}$$

Determination of the E-k dispersion relation in thin films of AlN from the tunneling J-V characteristics was proposed and carried out by Lewicki and co-workers[5,6,7,] in 1965. Padovani and Stratton[8] then extended the technique to Schottky barriers in a series of experiments on GaAs.

We have thus far treated only the low temperature case where a delta function of carriers at the conduction band minimum is a good approximation to the tunneling distribution. For practical reasons most of the measurements in the present work were made at 77°K and on semiconductors in the 10^{17} cm^{-3} carrier concentration range. This

combination of temperature and carrier concentration means that we must consider the thermal energy distribution of all of the carriers impinging on the barrier, integrated over the tunneling probability at those energies.

Padovani and Stratton[11] have shown that for values of s_o approaching q/kT the following correction to the exponent is necessary

$$\frac{d \log J}{dV} = s_o \tanh\left(\frac{q}{kT}\frac{1}{s_o}\right) \tag{11}$$

Since we are not far from the parabolic case the same correction can be applied to the two band calculation. Thus, for the two-band model the slope of the log J vs. V curve is given by

$$\frac{d \log J}{dV} = s \tanh\left(\frac{q}{kT}\frac{1}{s}\right) \tag{12}$$

where s is the bias voltage dependent slope defined by Eq. 7.

II.2 Effect of Trapping States

We will now consider the effect of trapping levels on the forward bias tunneling current. Since the tunneling probability is dependent on the width of the space charge region, this probability becomes quite small as the carrier concentration in the semiconductor is reduced. However, states in the forbidden gap can act as intermediate states and increase the tunneling probability under certain conditions.[16] The

situation can be analyzed in a manner analogous to that for recombination and generation through intermediate centers.[18,19,20]

Let us consider the following two-step process. In the forward direction, (1) the electron tunnels from the semiconductor conduction band to the state and then (2) from the state to the metal. If the concentration of states is N_t and f is the probability of occupation of the state by an electron then the number of unoccupied states is given by $N_t(1-f)$. Thus, from Fermi's Golden Rule the rates for the two processes are given by

$$R_1 = C_1 N_t (1-f) \exp\left\{-2\int_{x_o}^{x_1} k\,dx\right\} \tag{13}$$

and

$$R_2 = C_2 N_t f \exp\left\{-2\int_{x_1}^{x_2} k\,dx\right\}$$

where the factors C_1 and C_2 are slowly varying functions of the voltage, etc. The exponential represents the tunneling probability for each step. The limits on the integrals represent the transition steps as shown in Fig. 3.

Under steady state conditions, f will adjust itself until the two rates are equal. Thus

$$R_1 = R_2 = \frac{C_1 C_2 N_t \exp\left(-2\left\{\int_{x_o}^{x_1} k\,dx + \int_{x_1}^{x_2} k\,dx\right\}\right)}{C_1 \exp\left\{-2\int_{x_o}^{x_1} k\,dx\right\} + C_2 \exp\left\{-2\int_{x_1}^{x_2} k\,dx\right\}} \tag{14}$$

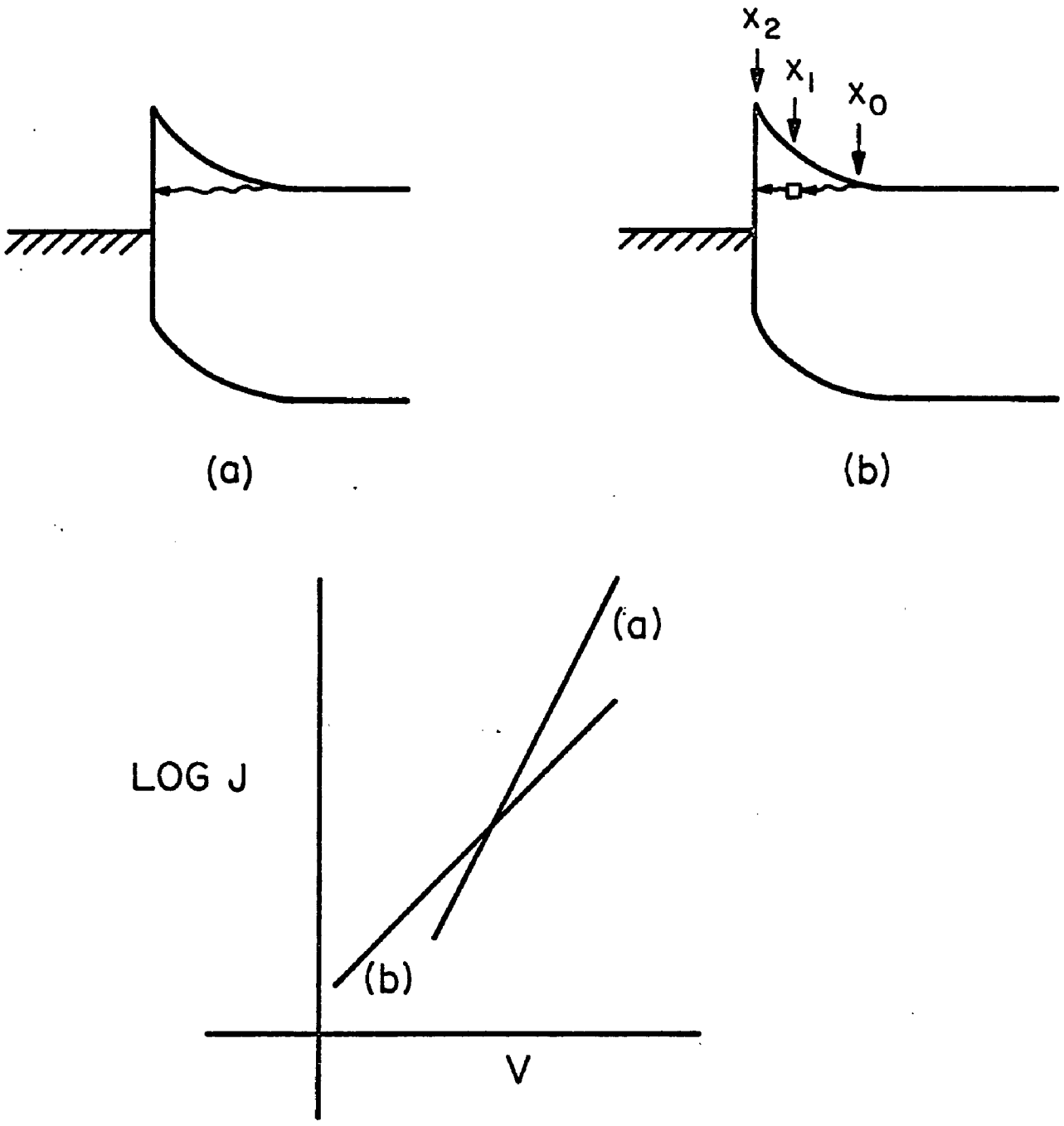

Fig. 3. Electron tunneling in the forward direction a) with and b) without an intermediate area. The J-V characteristics for each process are shown in c).

Equation 14 represents a peaked function of x_1 which, provided C_1 and C_2 are not too different, attains its maximum value when

$$\exp\left\{-2\int_{x_1}^{x_2} k\,dx\right\} = \exp\left\{-2\int_{x_o}^{x_1} k\,dx\right\} \tag{15}$$

If there are states available at the optimum value of x_1, the rate for the complete transition will be proportional to the peak value of Eq. 14 which is just the square root of the expression for single step tunneling

$$R \propto \exp\left\{-\int_{x_o}^{x_2} k\,dx\right\} \tag{16}$$

The number of traps and their distribution in energy will determine the magnitude and range over which Eq. 16 is valid. If states are available over a range of energies, we can repeat the procedure used in the preceding section and show that for the parabolic model the current is now of the form

$$J \propto \exp\left\{-\tfrac{1}{2}\, s_o(\phi_B - V + \xi)\right\} \tag{17}$$

The slope of the log J vs. V curves has been reduced to $\frac{1}{2}\, s_o$.* This analogous situation occurs in p-n junctions at low biases for the case of recombination via intermediate states in the space charge region. There the states change the slope of the log J vs. V curve from q/kT to $q/2kT$.

---

* This result is clearly independent of the detailed nature of E-k relationship.

For the present work on CdTe we have calculated the J-V characteristics as predicted by the two-band model with $E_g = 1.44$,[21] $\varepsilon = 10.7$,[21] and $m/m_e = 0.11$.[21] Figure 4 shows the results of the calculation plotted as log J vs. $-(\phi-V+\xi)$.

II.3 Reverse J-V Characteristics

For the reverse bias tunneling case, the electrons tunnel primarily from near the Fermi energy in the metal to the conduction band of the semiconductor as shown in Fig. 5. Unlike the forward bias case where there are no electrons available below the conduction band energy, states in the metal below the Fermi energy are filled and can contribute to the current. Like Padovani and Stratton[11] we will make the simplifying assumption that the electric field is nearly constant over the space charge region through which the electron tunneling takes place. Also we will define the electron energy to be zero when it reaches the conduction band edge. Thus, the electron energy as a function of distance from the metal is given by

$$\mathcal{E} = \phi_B - E_m x \tag{18}$$

where E_m is the maximum electric field in the space charge region.

Differentiating and substituting Eq. 1 for the maximum electric field, we find

$$\frac{d\mathcal{E}}{dx} = -\sqrt{\frac{2qN_D}{\varepsilon}(\phi_B+\xi-V)} \tag{19}$$

and hence the tunneling current is given by

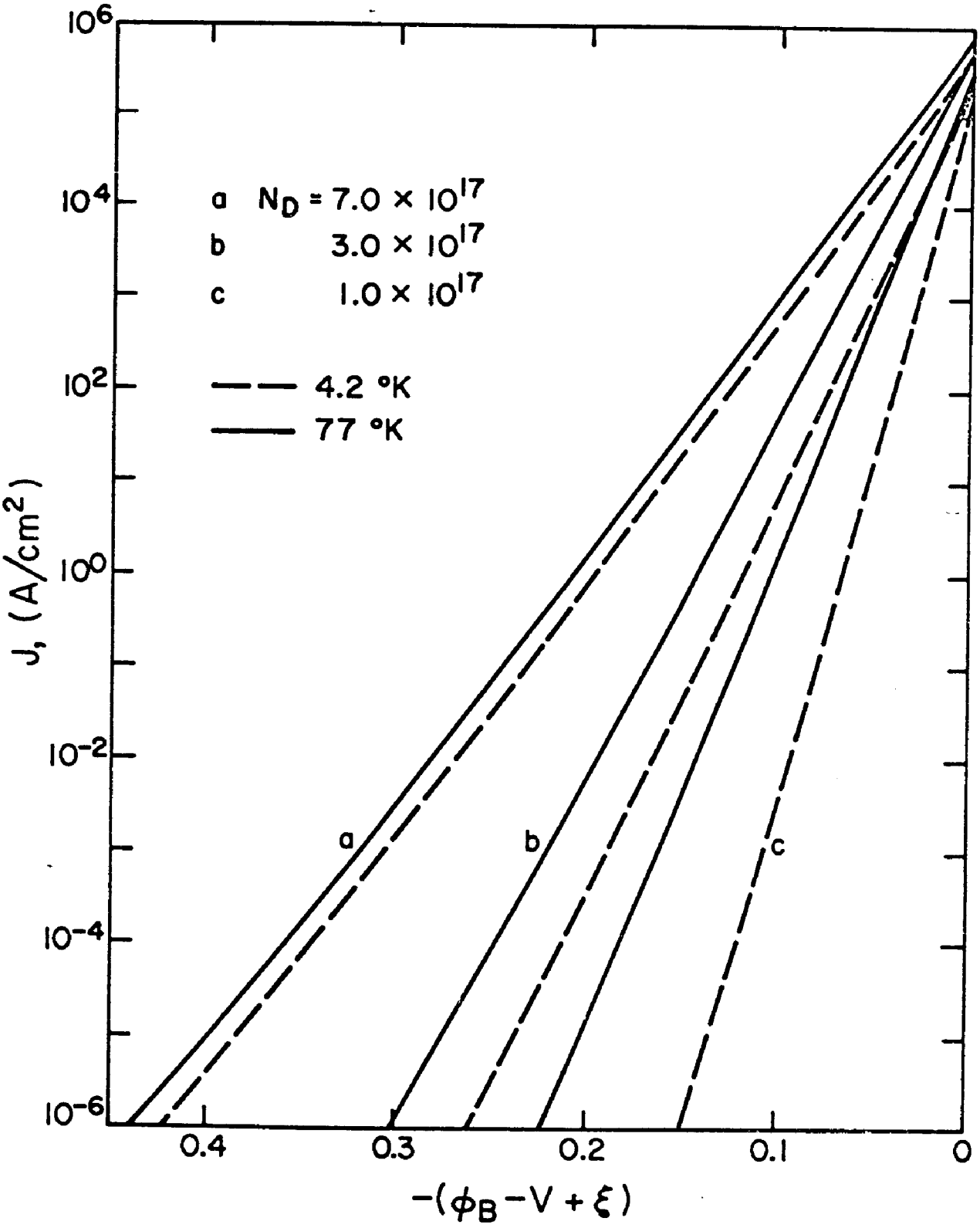

Fig. 4. Theoretical tunneling characteristics for a forward biased Schottky barrier based on the two-band model given by Eq. 7.

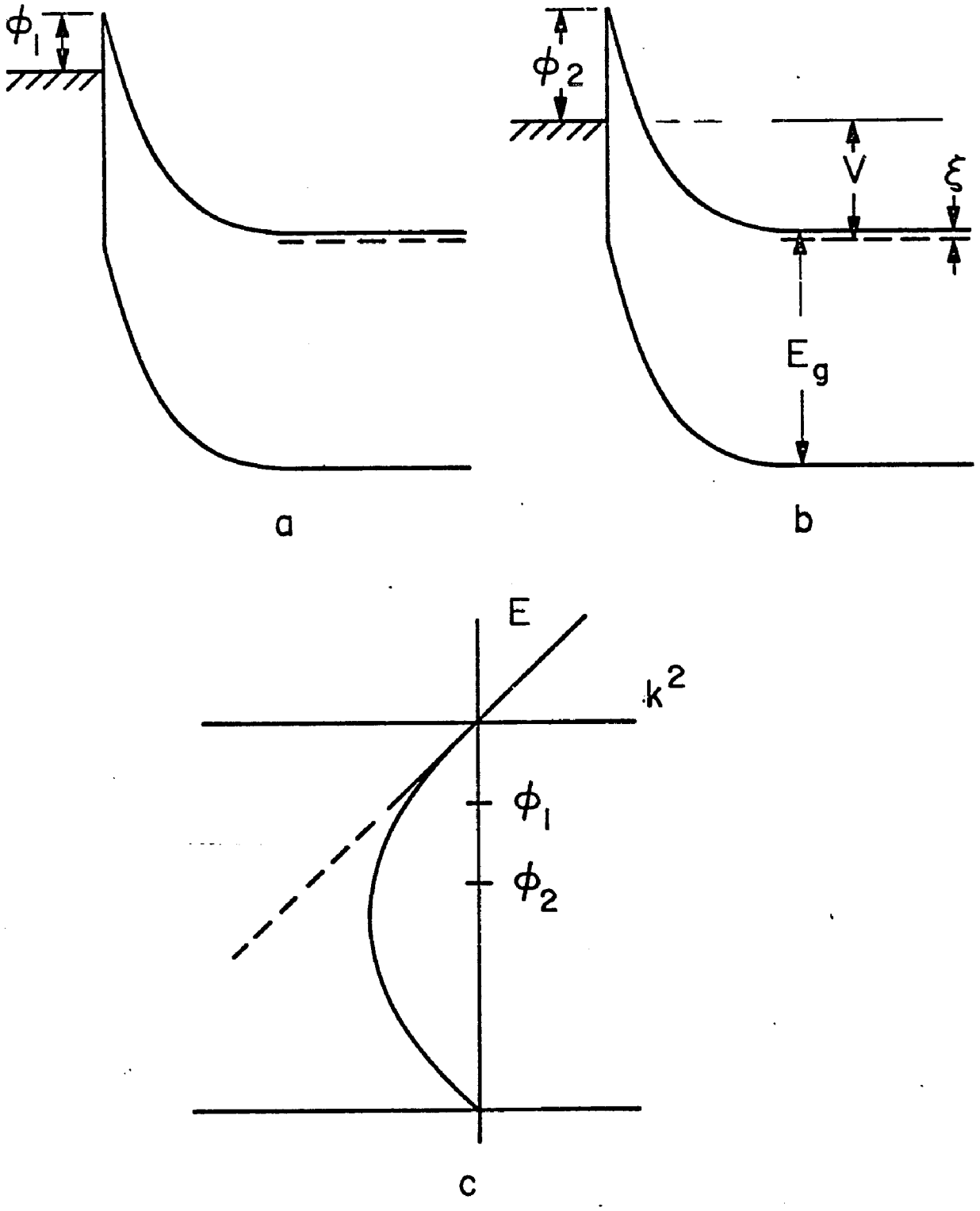

Fig. 5. Reverse bias electron tunneling from the metal to the semiconductor for two different barrier energies, showing the different range of k involved in the two cases.

$$J = J_s \int_{\infty}^{\infty} f(\hat{\mathcal{E}})\, d\hat{\mathcal{E}} \exp\left\{ -2 \int_{\phi_B}^{0} \frac{dx}{d\hat{\mathcal{E}}}\, k(\hat{\mathcal{E}})\, d\hat{\mathcal{E}} \right\} \tag{20}$$

where $f(\hat{\mathcal{E}})$ is the electron distribution in the metal. Using the supply function of Murphy and Good,[22] Eq. 20 can be written in the form

$$J = J_s \left(\phi_B + \xi - V\right) \exp 2\left\{ \sqrt{\frac{\varepsilon}{2qN_D}}\ \frac{1}{\sqrt{\phi_B+\xi-V}} \int_{\phi_B}^{0} k(\hat{\mathcal{E}})\, d\hat{\mathcal{E}} \right\} \tag{21}$$

where

$$J_s = \frac{m^*}{2\pi^2} \left(\frac{q}{\hbar}\right)^3 s_o^{\,2}$$

Equation 21 is in agreement with that presented by Padovani and Stratton[11] for the low temperature case.*

In the forward bias case, it is possible to differentiate the log J vs. V curve and obtain the E-k relation directly, because the range of k depends upon the applied voltage. However, in reverse bias, the range of k is essentially independent of applied voltage; and, by differentiating the reverse bias log J vs. V curves, one can determine only the integral over k as follows:

*For the carrier concentrations in the present work these expressions are valid at 77°K.

$$\frac{d \log J_m \frac{J}{(\phi_B+\xi-V)}}{d \frac{1}{\sqrt{\phi_B+\xi-V}}} = \sqrt{\frac{\varepsilon}{2qN_D}}\, 2\int_{\phi_B}^{\infty} k(\mathcal{E})\, d\mathcal{E} \qquad (22)$$

Thus, for any given barrier energy a plot of log $\frac{J}{\phi_B+\xi-V}$ vs. $\frac{1}{\sqrt{\phi_B+\xi-V}}$ will yield a straight line whose slope depends on carrier concentration, barrier energy, and the k integral. By varying the barrier energy (through the use of different metal barriers), one can determine the variation of the integral over k and compare the results with theoretical models.

Chapter III

Experimental Results in CdTe Schottky Barriers

III.1 Sample Preparation

The CdTe crystals cleave readily on the $\langle 110 \rangle$ crystal planes, thereby making it possible to obtain large flat surface areas. Surfaces obtained in this manner are, of course, free of contaminants introduced by chemical cleaning procedures. It is also possible to cleave the crystal in an evaporating stream of metal in a vacuum thereby further reducing the possibility of surface contaminants.

A special fixture was constructed to cleave the crystal in a vacuum and cover it with a metal mask. The mask was spring loaded such that it covered the crystal immediately upon cleaving. The entire procedure was carried out in an ion pumped vacuum system at 10^{-7} Torr.

Alternatively the CdTe may be cleaved in air and then immediately placed in a vacuum system. This technique allows selection of the best cleaved surfaces. Typical diodes were 10^{-2} cm diameter. The only differences between the vacuum cleaved and the air cleaved samples were slightly higher values for the barrier energy on the latter (as determined from capacitance vs. voltage measurements) which seemed to have no effect on the slope of the log J vs. V curves. The effect did, however, correlate with corresponding decreases in the J_o, or zero bias intercept, obtained by extrapolation of the log J vs. V curves. All of the samples used in the reverse bias tunneling measurements were vacuum cleaved to insure an intimate metal-semiconductor contact.

Back contact to the samples consisted of In-Ag solder which was

alloyed prior to cleaving. The crystals were cut from two different CdTe ingots which subsequently led to different observed characteristics. Metals of different electronegativities were evaporated to produce a range of barrier energies. The results are given in Table I with their corresponding barrier energy as measured from capacitance voltage characteristics on the vacuum cleaved samples. The J-V characteristics of the completed diodes were measured at room temperature both in the forward and reverse directions. Also the carrier concentration and diffusion potential were determined from $(\text{capacitance})^{-2}$ vs. voltage plots. The error in N_D was estimated to be ±10%, resulting mainly from the uncertainty in the area of the sample. The diodes were then immersed in liquid nitrogen and the measurements repeated. A special probe assembly was constructed to permit measurements at 4.2°K by lowering the sample into a storage dewar filled with liquid helium. The slope of the $(\text{capacitance})^{-2}$ vs. voltage curve for any given sample remained unchanged (within 5%) at all three temperatures.

III.2 Forward J-V Characteristics

The room temperature J-V characteristics followed the usual diode equation:

$$J = J_o \left\{ e^{qV/nkT} - 1 \right\} \tag{23}$$

where the parameter n[23] took on a value of 1.1. The use of several different metals for the Schottky barriers produced a range of barrier energies which permitted the consistency of the results to be checked. Figure 6 shows capacitance-voltage data on material of the same carrier concentration for three metals. The forward log J-V characteristics

Table I

Metal	ϕ_B (Cap)
Al	.35 ± .02 eV
Mg	.40
In	.50
Ni	.53
Cu	.57
Ag	.65
Pd	.65
Au	.69

Table I. The barrier energy of various metals on n-type CdTe as determined from (capacitance)$^{-2}$ vs. voltage plots.

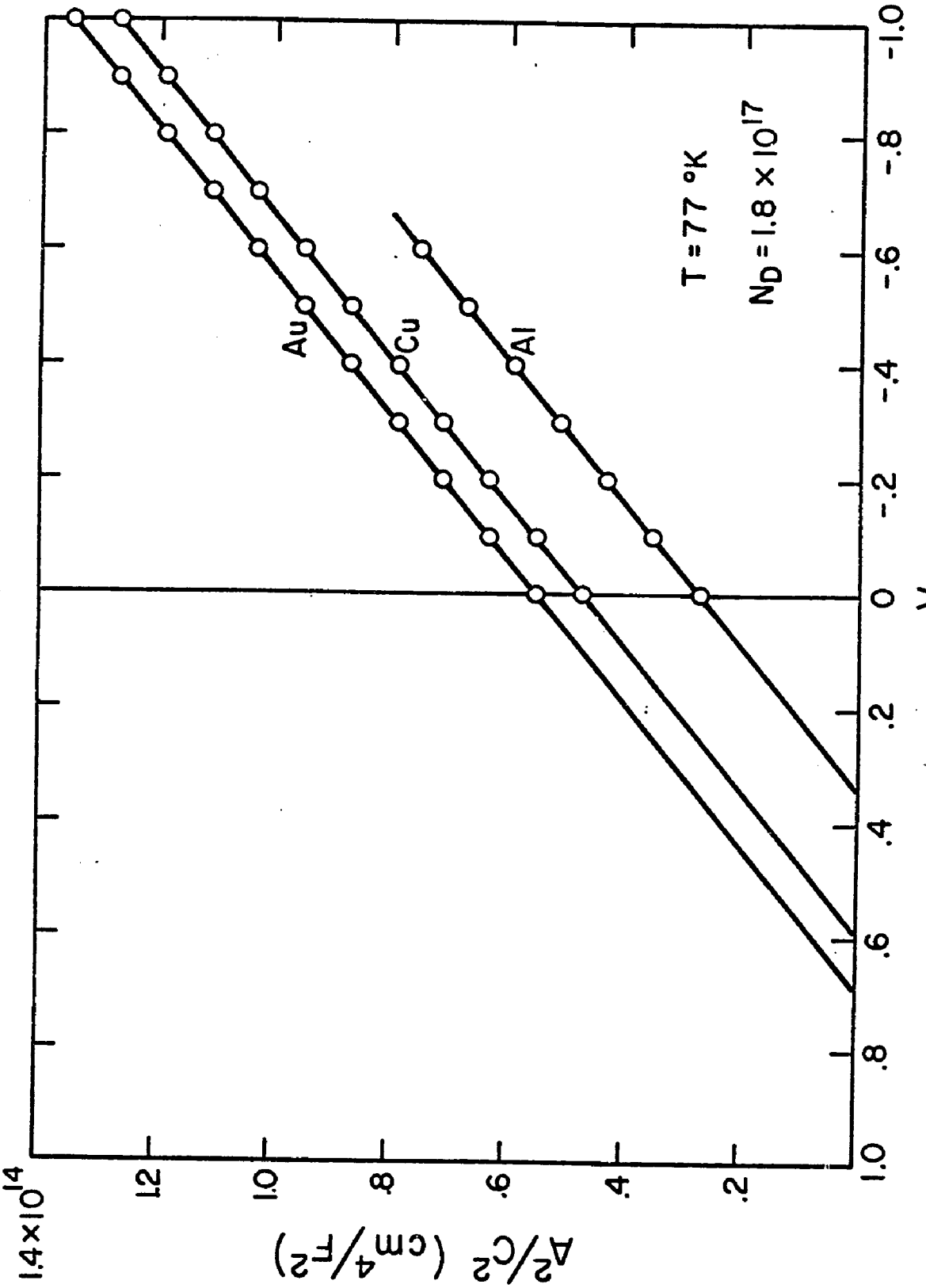

Fig. 6. Capacitance-voltage plots of Au, Cu, Al Schottky barriers on n CdTe.

for these samples taken at 77° K are illustrated in Fig. 7. The curves have the same slope but are displayed by exactly the difference in barrier energies as expected from Fig. 6. The slope of these curves changed very little at 4.2° K thereby giving assurance that the observed current is indeed the result of electron tunneling through the barrier. A selection of samples cut from different portions of an ingot of CdTe provided a range of carrier concentrations. According to Eq. 6, variations in carrier concentration should be reflected in the slope of the low temperature log J vs. V curves. Figure 8 illustrates the tunneling characteristics of Schottky barriers of the same energy for several carrier concentration levels in the CdTe. The log J vs. V curves exhibit two distinct regimes, whose slopes differ by a factor of 2. The upper regime is in agreement with the calculation based on the parabolic model given by Eq. 6 whereas the lower regime is attributable to tunneling of electrons via an intermediate state (Eq. 17).

A second group of diodes was similarly fabricated from a different ingot of CdTe and the above procedure repeated. The J-V characteristics as illustrated in Fig. 9 now show only a single regime which correlates with the intermediate state tunneling calculation (Eq. 17). These results were not surprising in view of the fact that this particular ingot was prepared in such a manner that it was expected to have a high density of shallow trapping centers.

The wide range of energy over which tunneling occurred via intermediate states can be attributed to thermal broadening of the peak of Eq. 14 at 77° K. The diode J-V characteristics began to exhibit structure when the samples were cooled to near liquid helium temperatures,

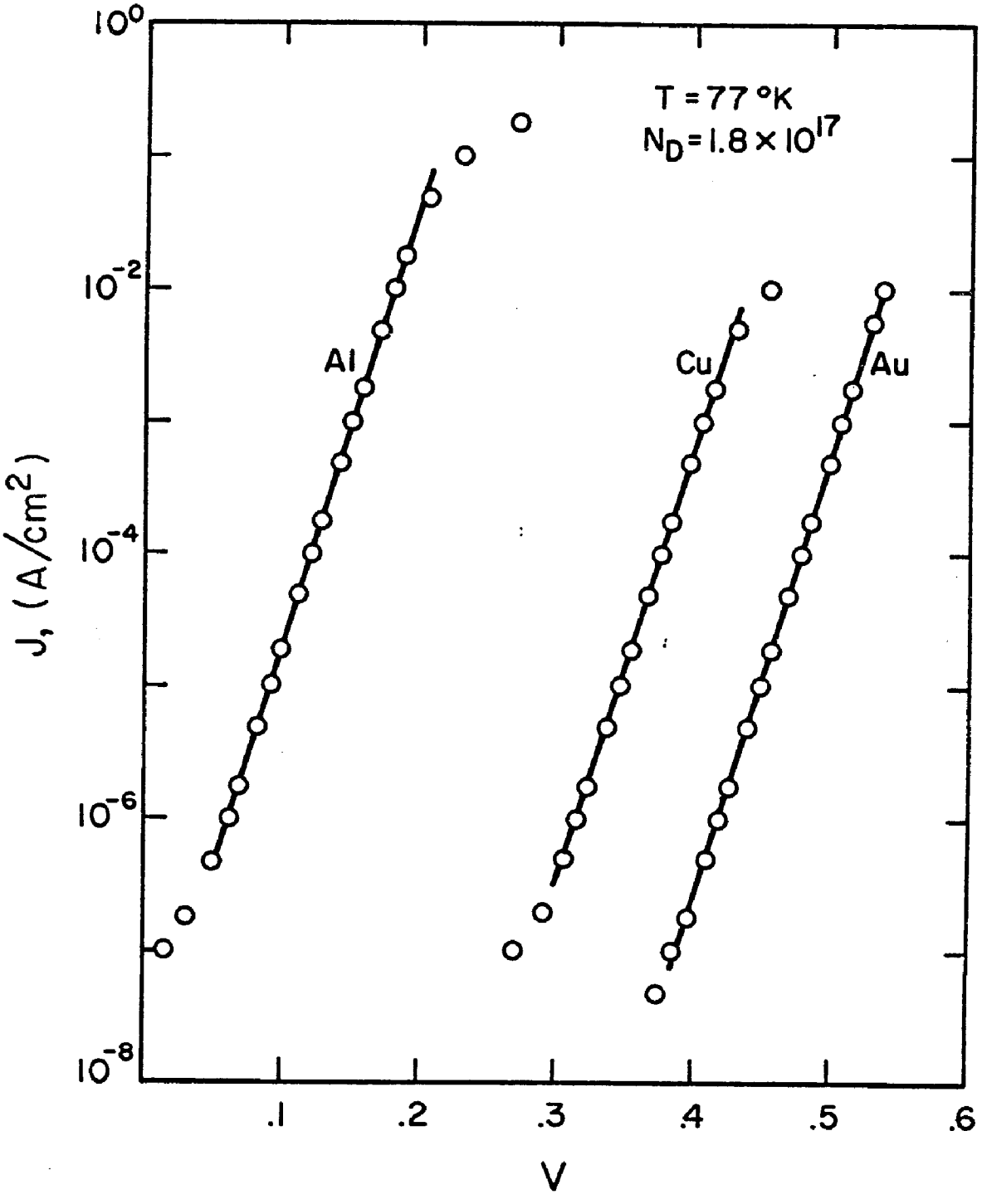

Fig. 7. Tunneling J-V characteristics of Au, Cu, Al Schottky barriers on n CdTe illustrating the shift resulting from their different barrier energies.

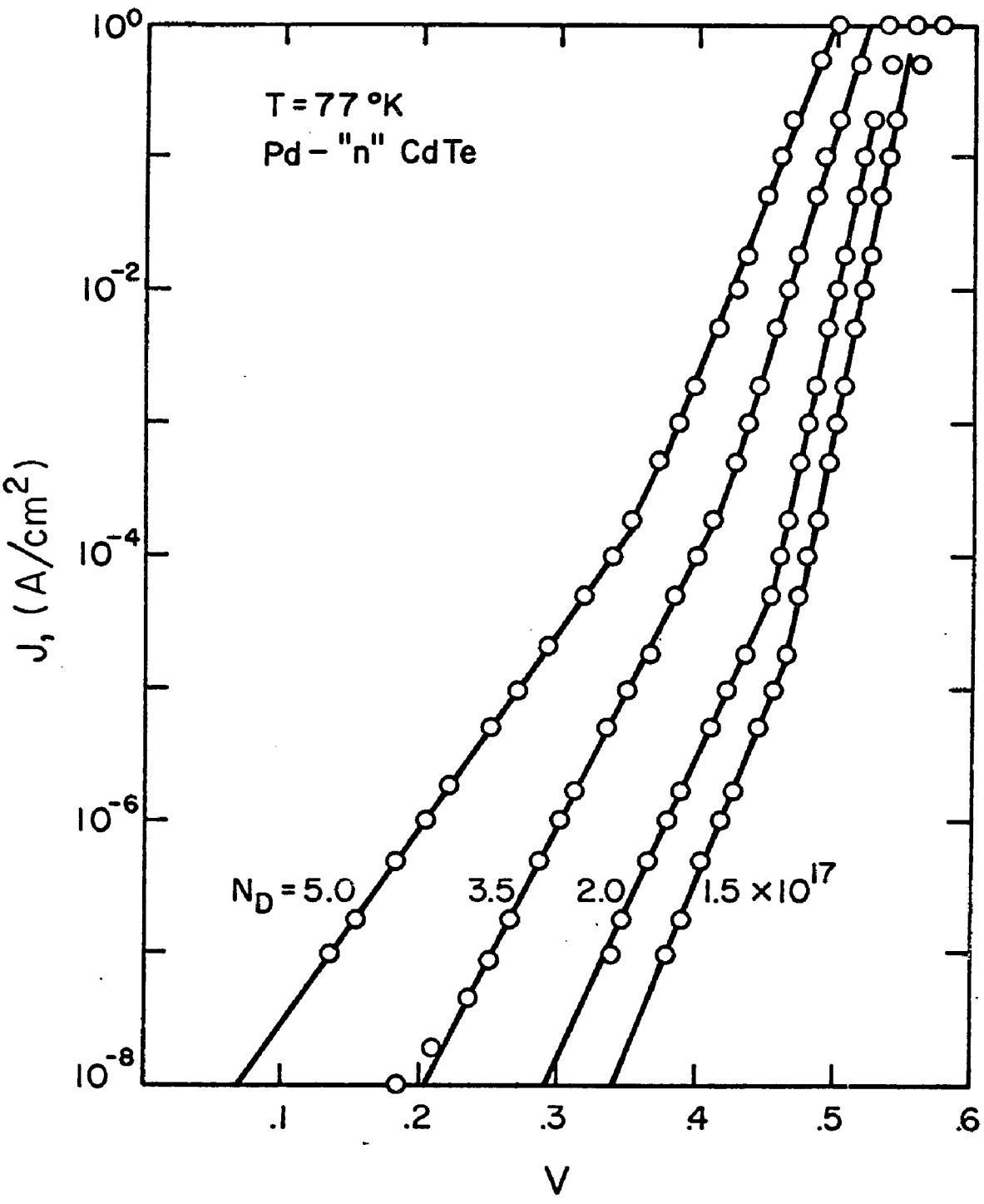

Fig. 8. Forward bias J-V characteristics of Pd Schottky barriers on n-type CdTe samples of several carrier concentrations. The upper slopes correspond to the simple tunneling theory (Eq.6) while the lower slopes correspond to tunneling through an intermediate state (Eq.17).

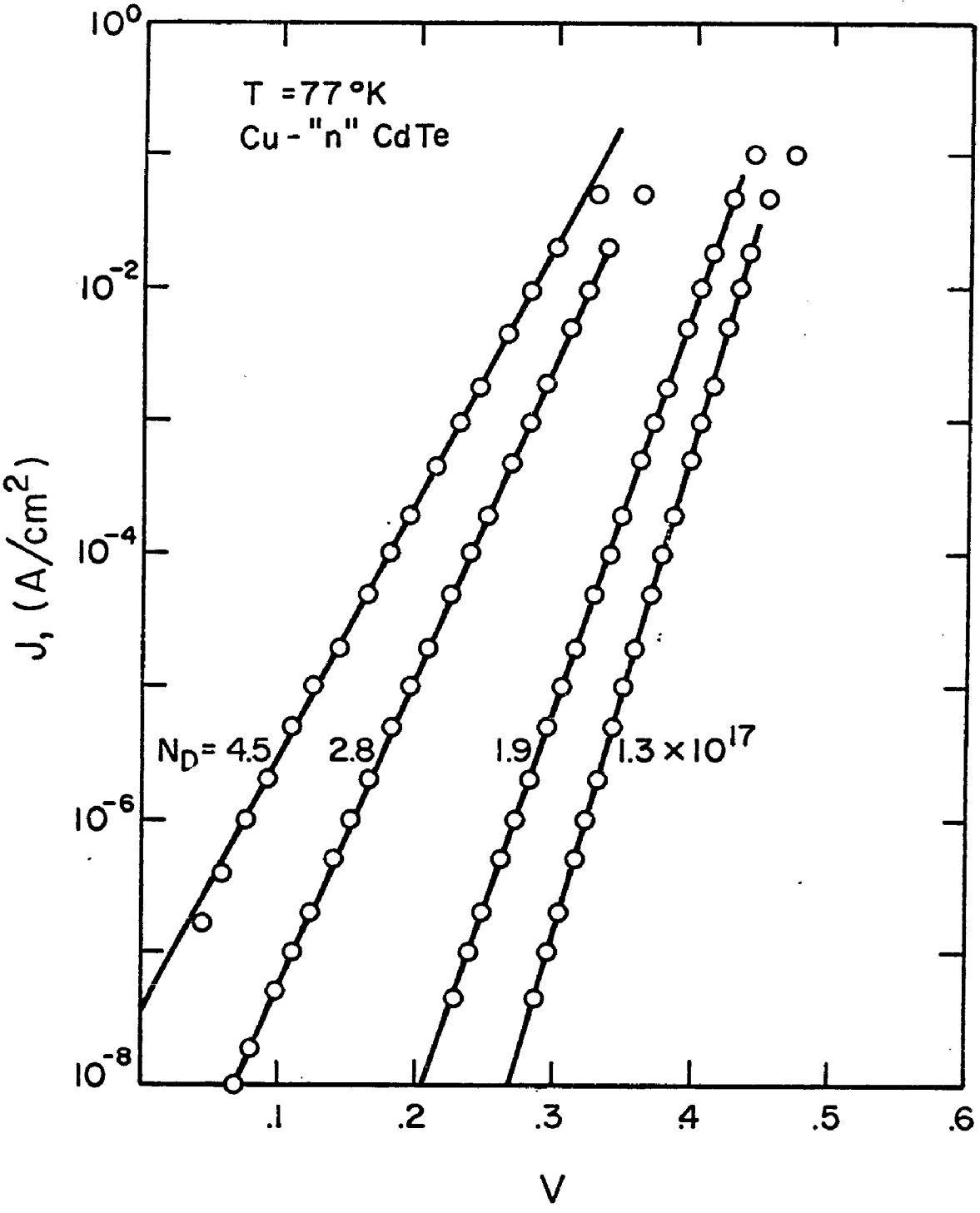

Fig. 9. Tunneling J-V characteristics of Cu Schottky barriers on n-type CdTe samples of different carrier concentrations.

thus confirming that trapping states are responsible for the observed behavior. Figure 10 shows a typical characteristic taken at 77° K and $\simeq 10^{\circ}$ K.

The dual slope behavior which was observed in these tunneling measurements is analogous to that observed in the forward J-V characteristics of p-n junction diodes in silicon and gallium arsenide.[18] There the dual slope is attributable to the recombination in the space charge region at small applied bias and to minority carrier injection at larger forward bias.

We believe that the effect of traps on tunneling have not been identified before because in most tunneling measurements large carrier concentrations are used to obtain high tunneling probabilities. Thus, the magnitude of the single tunneling step current would be greater than that expected for tunneling through intermediate states. However, in barriers on low carrier concentration materials excess currents are frequently observed and have not been understood.[24] In these later cases tunneling through traps may be involved.

The possibility of an edge effect contribution to the observed J-V characteristics was investigated in two ways. First, dots of two different areas were evaporated onto two opposing freshly cleaved crystal faces. The current at any given voltage was directly proportional to the area while the slope of the log J vs. V curve remained the same. Second, 0.02 cm diameter dots of aluminum were evaporated onto a cleaved crystal. Then after measuring the J-V characteristics, 0.04 cm diameter dots of gold were evaporated, centered over the aluminum dots. The J-V characteristics of these new structures showed no change in the

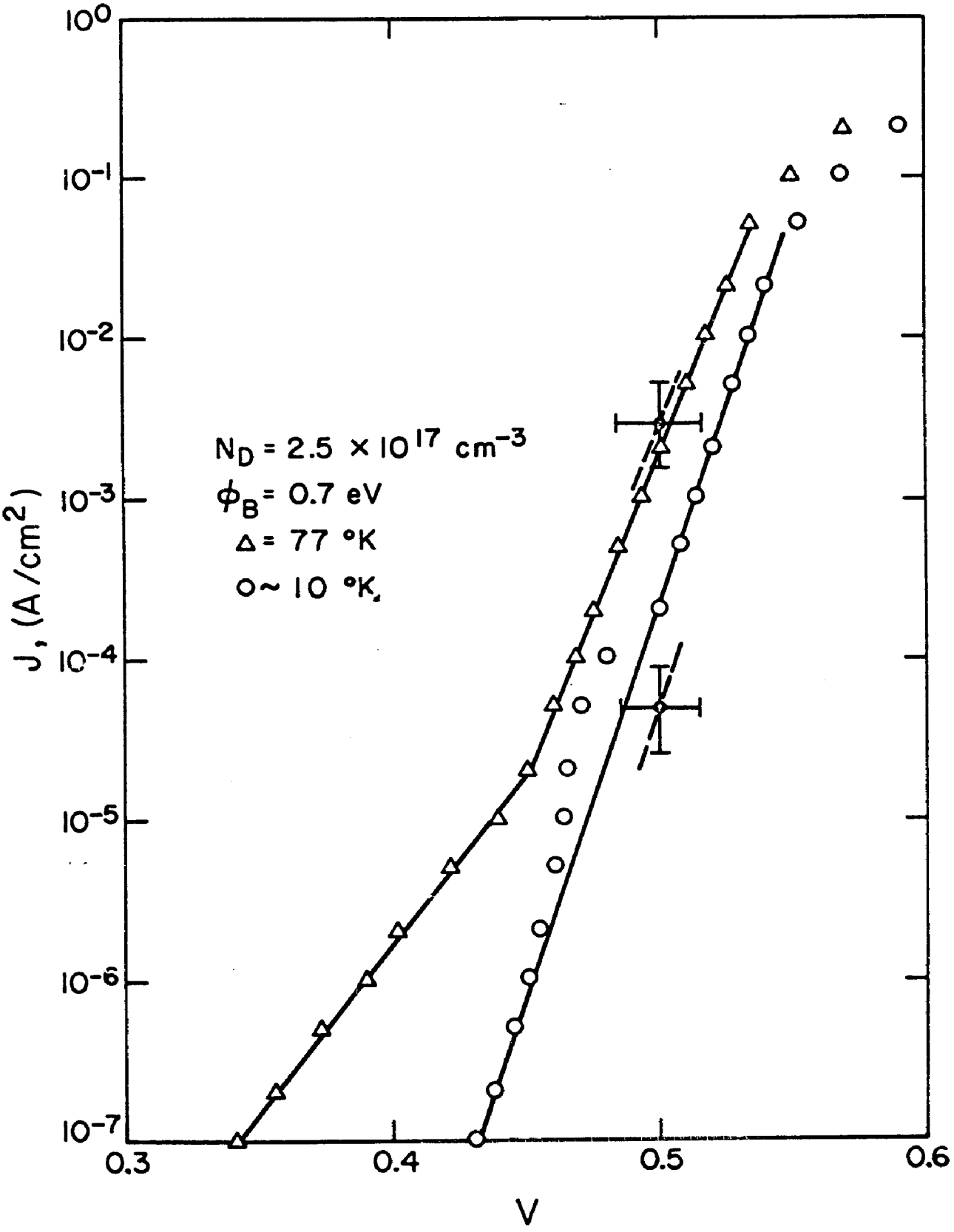

Fig. 10. Tunneling J-V characteristics showing the effects of traps at 77° K and at 10° K. The theoretical magnitude of the tunneling current is also shown.

range of interest. Since the Al-CdTe barrier energy is .35 volts and the Au-CdTe barrier energy is .69 volts, the current to be expected from a gold barrier is many orders of magnitude below that observed on the aluminum barrier. Thus, we can conclude that the perimeter of the metal dots does not make a noticeable contribution to the J-V characteristics.

The limited range of forward bias voltage (or energy) over which the tunneling current is unambiguously observed in the present diodes does not enable us to distinguish between the parabolic and the two-band E-k dispersion relation. Thus, we have taken the tunneling log J-V curves as straight lines which are characteristic of the parabolic model. The slopes of these straight lines are presented in Fig. 11 as a function of carrier concentration for the diodes exhibiting both one and two regimes. Curve A represents the computed value of s_o as a function of carrier concentration and is thus the slope of the log J vs. V curves for the parabolic model neglecting thermal effects. Curve B represents the slope as computed from the two-band model and evaluated at $\phi_B + \xi - V = 0.150$ volts; a typical bias condition at which the slope would be measured. Curves C and D have included the temperature dependence at 77^o K for the two models as expressed in Eqs. 11 and 12. Curve E shows the case of tunneling via an intermediate state and is plotted as $s_o/2$ vs. $1/N^{1/2}$. Good agreement between the observed and calculated slopes is obtained in all cases.

To this point we have concerned ourselves primarily with the exponent or slope of the log J-V curves. For completeness, the pre-exponential terms of Eq. 6 have been evaluated for the diode characterized

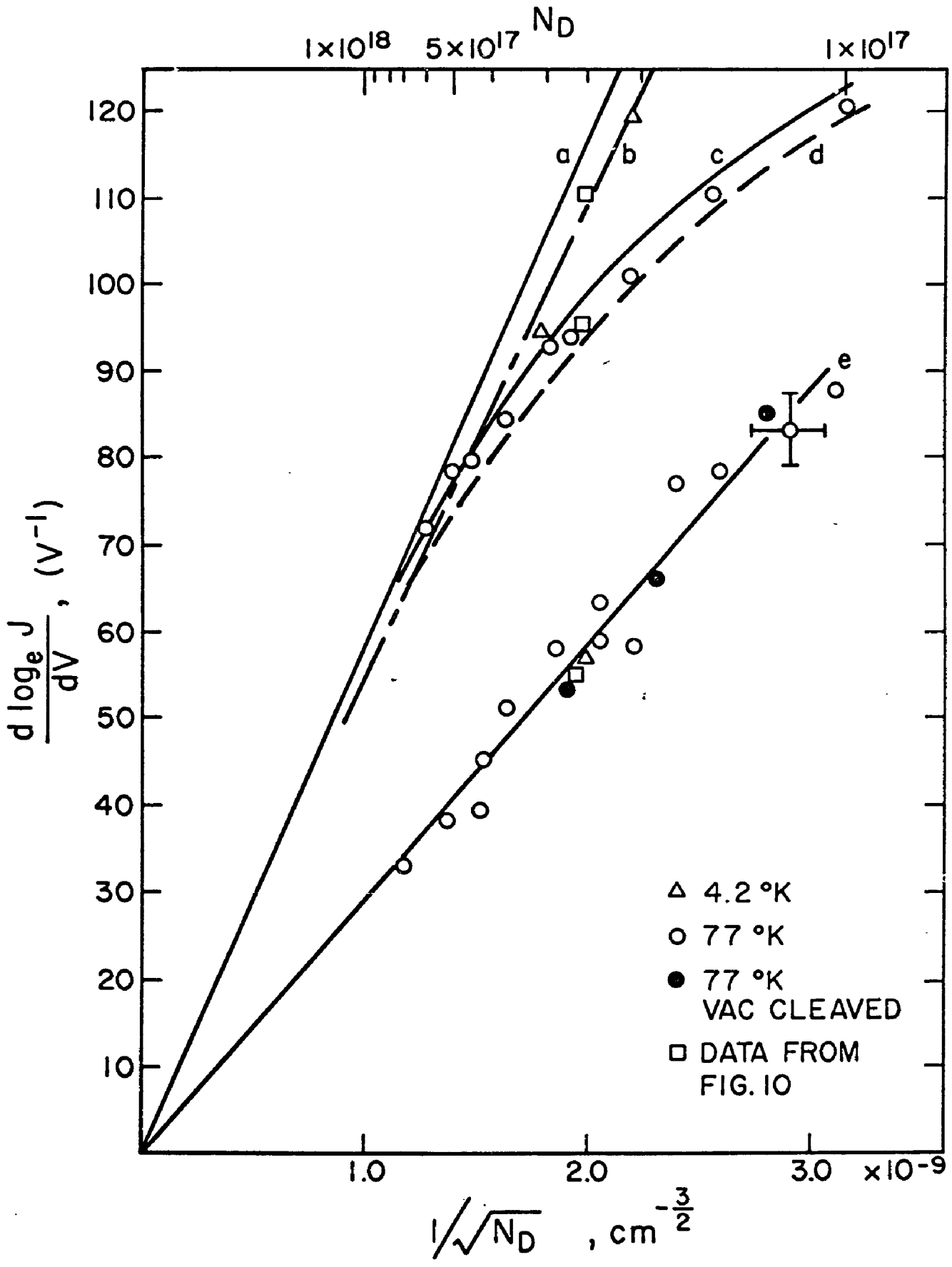

Fig. 11. (see page 33)

Fig. 11. Slope of the forward bias log J-V tunneling curves as a function of carrier concentration. Experimental points are taken from curves such as Figs. 7, 8, and 9.

a) theoretical curve based on parabolic band model at 4.2° K.

b) two-band model at 4.2° K and evaluated at $(\phi_B - V + \xi) = .150$ V .

c) parabolic model at 77° K .

d) two-band model at 77° K, $(\phi_B - V + \xi) = 0.150$ V .

e) parabolic model for tunneling via an intermediate state at 77° K . Theoretical curves were computed from the published value[21] of the effective mass and contain no adjustable parameters.

in Fig. 10. The theoretical magnitude of the currents has been computed at the two points indicated. Excellent agreement is obtained within the uncertainty in the values for barrier energy and carrier concentration used in the calculation.

We have concluded that trapping states are responsible for the observed departures from theory. It is possible to determine the energy location of these centers for the particular junction characterized in Fig. 10. The J-V characteristic at 10^{o} K indicates a peak at $\phi_B - V + \xi = .22$ eV . From Eq. 15 we know that at the peak

$$\int_{x_o}^{x_1} k dx = \int_{x_1}^{x_2} k dx \tag{24}$$

Since we are close to the conduction band, the parabolic model for the dispersion relation is adequate. Thus

$$\int_{o}^{E_t} s_o dE = \int_{E_t}^{\phi_B - V + \xi} s_o dE \tag{25}$$

and

$$E_t = \tfrac{1}{2}(\phi_B - V + \xi) \tag{26}$$

or 0.11 eV for the present case.

Next we wish to estimate the density of traps needed to account for the tunneling behavior presented in Fig. 10. At the transition between the upper and lower slope the tunneling currents for the two step and one step process are equal. We can estimate the spatial thickness,

Δx , of the layer of traps acting as intermediate states by the distance necessary to reduce the tunneling probability by $1/e$. At the transition point $\Delta x \cong \frac{2}{k} = 36$ Å . Since the two currents are equal, the total cross sectional area of the participating states must equal the ratio of their respective tunneling probabilities or:

$$\frac{\sigma N_t}{\Delta x} \exp\left\{-\frac{s_o}{2}(\phi_B - V + \xi)\right\} = \exp\left\{-s_o(\phi_B - V + \xi)\right\} \qquad (27)$$

where σ is the capture cross section and N_t the density of traps. Evaluating Eq. 27 at $\phi_B - V + \xi = .22$ V using a capture cross section of 50 Å^2 , we find a trap density of 1.5×10^{15} cm^{-3} . This density is typical of those normally encountered in II-VI Compounds.[25]

III.3 Reverse J-V Characteristics

In the case of the forward bias characteristics, a change in barrier energy merely moved the log J vs. V curves horizontally on the voltage axis. However, under reverse bias in addition to being displaced horizontally the slope also changes. Figure 12 shows four log J-V curves for diodes of different barrier energies. On CdTe having an N of 3.6×10^{17} cm^{-3} from Eq. 22, we see that if we plot

$$\log \frac{J}{(\phi_B + \xi - V)} \text{ vs. } \frac{1}{\sqrt{\phi_B + \xi - V}}$$

the result should be a straight line. The slope of the curves will then give a value for the integral of k over the energy range from the barrier energy to the conduction band. Data taken from Fig. 12 have been replotted in this manner in Fig. 13.

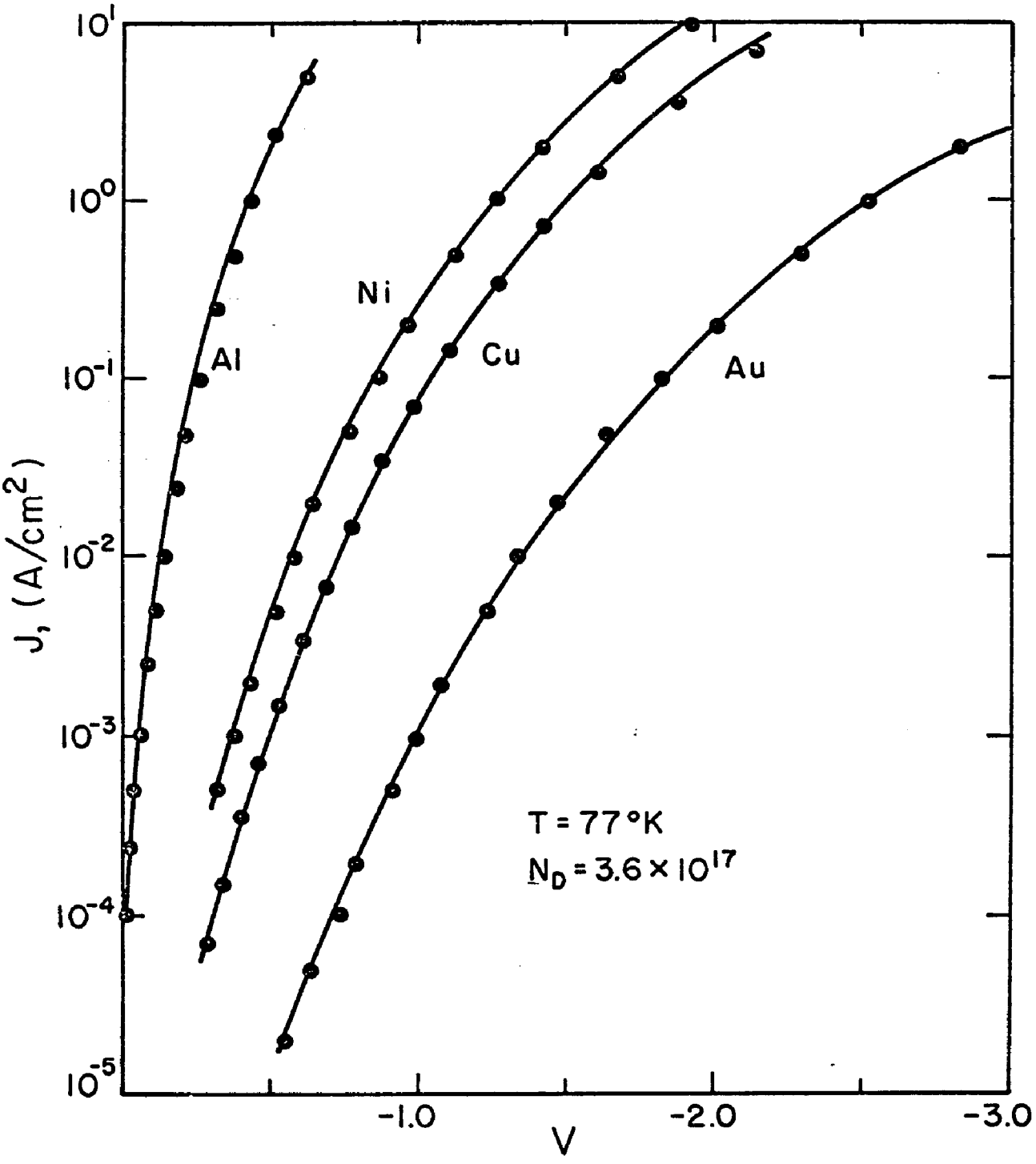

Fig. 12. Reverse bias tunneling characteristics of four Schottky barriers of different barrier energies on n CdTe.

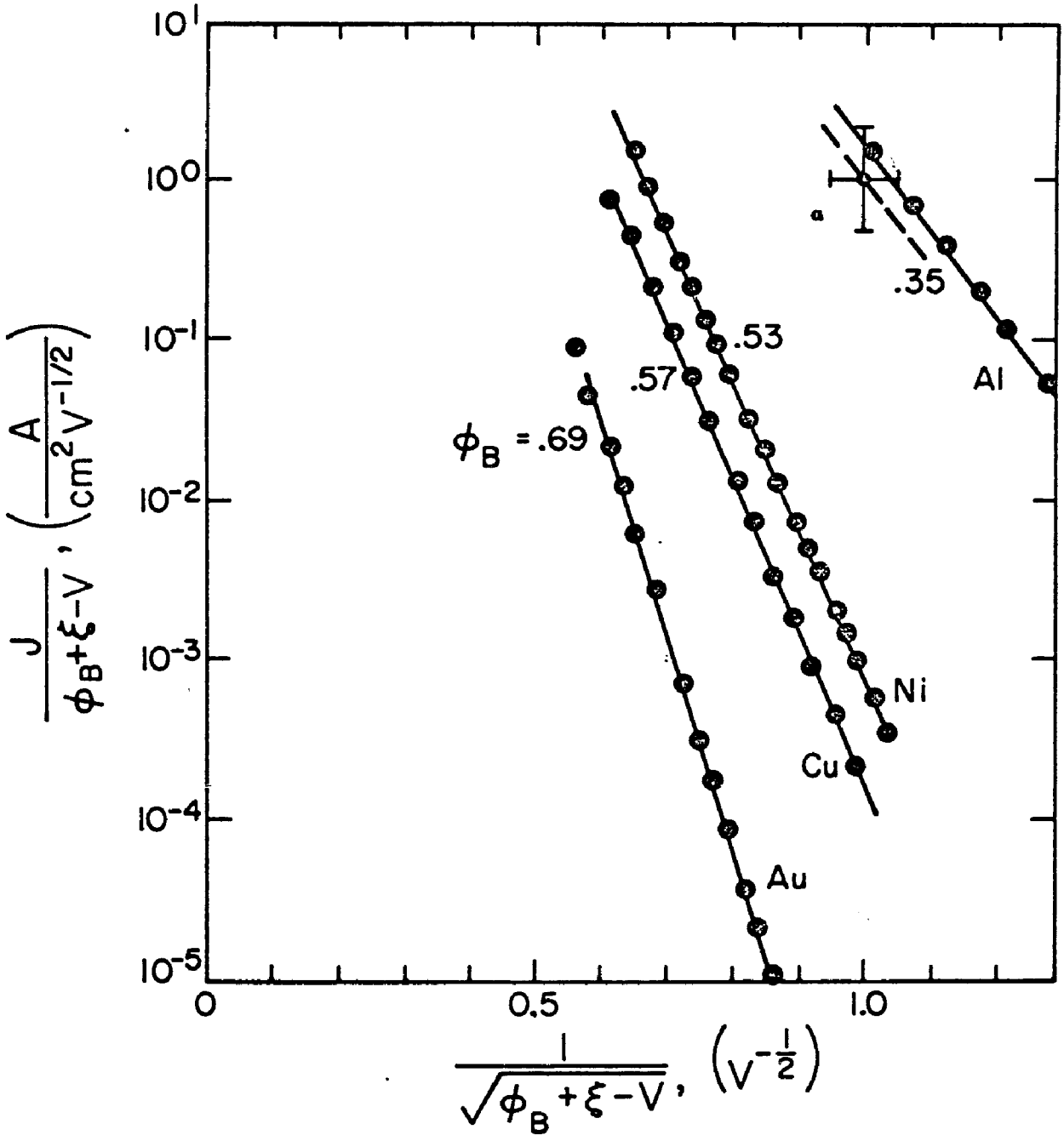

Fig. 13. A Fowler-Nordheim type plot of the data of Fig. 12 showing systematic variation of slope with barrier energy. The point a represents the theoretical magnitude predicted by Eq. 22.

We have included the theoretical value of $J/(\phi_B-V)$ on Fig. 13 for the Al barrier evaluated at $(\phi_B-V) = 1$ V using Eq. 22 where the integral over k was evaluated based on the two-band model. The error bars again represent the uncertainties in barrier energy and carrier concentration. The other curves were similarly compared and all found to agree within these error limits. Figure 14 then shows the integral of k vs. barrier energy inferred from the slopes of these curves. We have plotted for comparison the theoretical values for the parabolic and two-band model with $N = 3.6 \times 10^{17}$ cm^3 . The experimental points are also normalized to this value of carrier concentration. Five to ten samples were fabricated with each of the metals indicated and the data points which are plotted represent the average value of those measured. The error bars indicate the deviation and are the result of the uncertainty in the measurement of barrier energy and carrier concentration by the capacitance-voltage techniques described earlier. These data clearly indicate that the E-k dispersion relation in the forbidden gap in CdTe is in good agreement with the two-band model. Several samples were also measured at $4.2^{\circ}K$ and the results were in agreement with those obtained at $77^{\circ}K$.

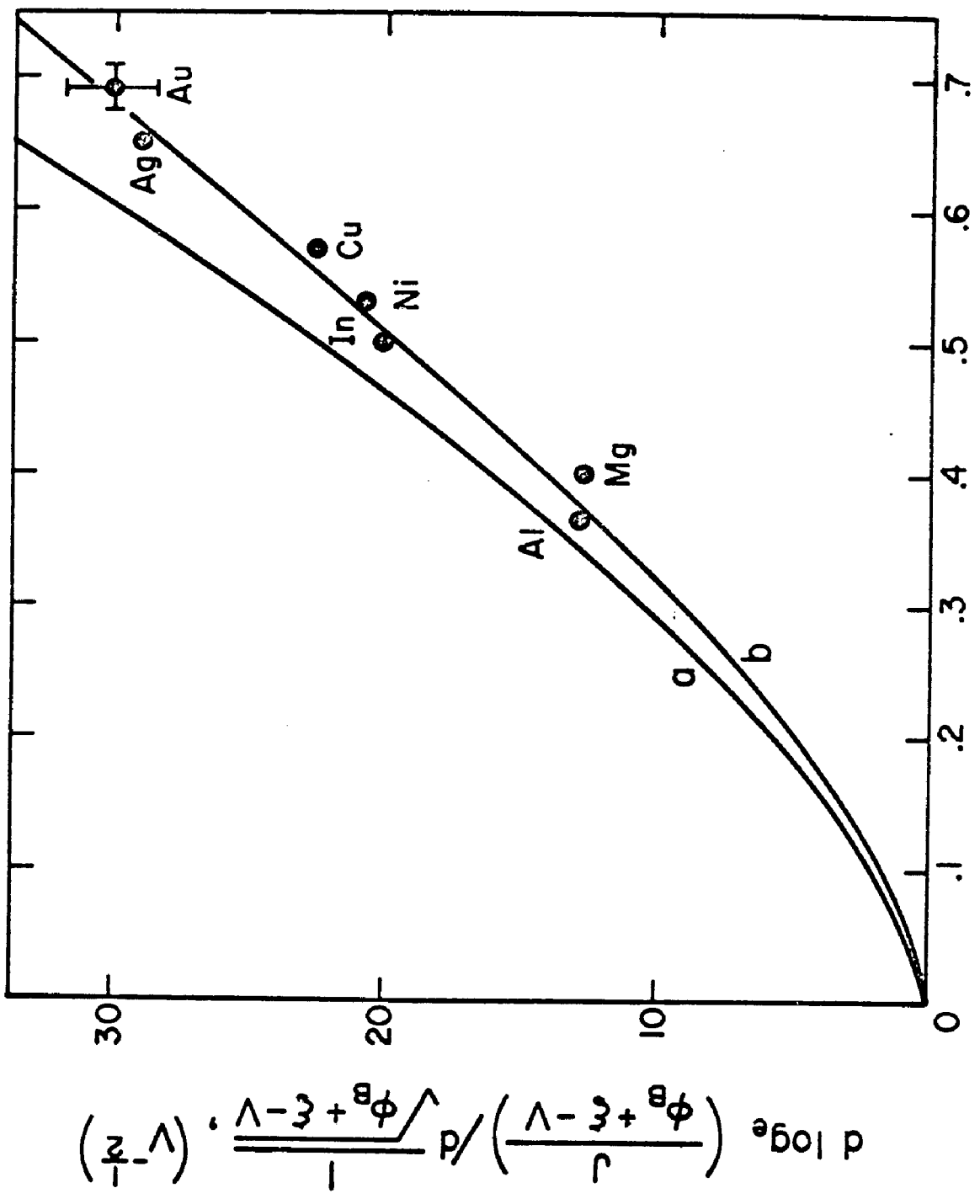

Fig. 14. A plot of the integral of k from the Fermi energy in the metal to the semiconductor conduction band for a) the parabolic model and b) the two-band model as a function of barrier energy. The experimental points are those obtained from the slopes of the curves like those of Fig. 13. (N_D=3.6x10^{17})

Chapter IV

Experimental Results in InAs Schottky Barriers

InAs samples were prepared by two techniques:

(a) Crystals were cleaved in air quickly placed on a metal mask in a Vac-Ion system. The chamber was evacuated to approximately 10^{-7} Torr and metal dots evaporated on the cleaved surface through the mask. The typical sample was exposed to air less than 30 sec prior to pump-down.

(b) Crystals were cleaved in vacuum in an evaporating stream of metal. After completion of the evaporation, the samples were removed from the vacuum, masked with either black wax (for single dots) or photoresist (for guard-ring structures) and the remaining metal etched away.

No systematic differences were found between samples formed by the two techniques. A summary of the sample characteristics are given in Table II. Typical forward current-voltage curves taken with the samples immersed in liquid nitrogen are shown in Fig. 15.

Although in principle a semiconductor may be characterized over a substantial energy range by tunneling measurements on a single sample, in practice the range of accurate data obtained is limited at very low current levels by leakage and at high forward bias by series resistance. For this reason it is necessary to use material of high carrier concentration (and hence large tunneling current) for measurements at low biases. With material of somewhat lower concentrations, the tunneling current is reduced and considerably higher forward bias may be applied

Sample	Metal	Preparation	(eV)	Area (cm^2)	N (10^{17} cm^{-3})
1	Au	Air cleave	0.51	7.5×10^{-5}	6
2	Cu	Air cleave	0.38	7.5×10^{-5}	1.6
3	Cu	Air cleave	0.38	7.5×10^{-5}	1.6
4	Al	Vacuum cleave	0.38	3.8×10^{-4}	1.6
5	Al	Vacuum cleave guard ring	0.38	1.6×10^{-5}	1.6

Table II. Characteristics of samples used in the E-k analysis. Sample numbers correspond to those in Fig. 15.

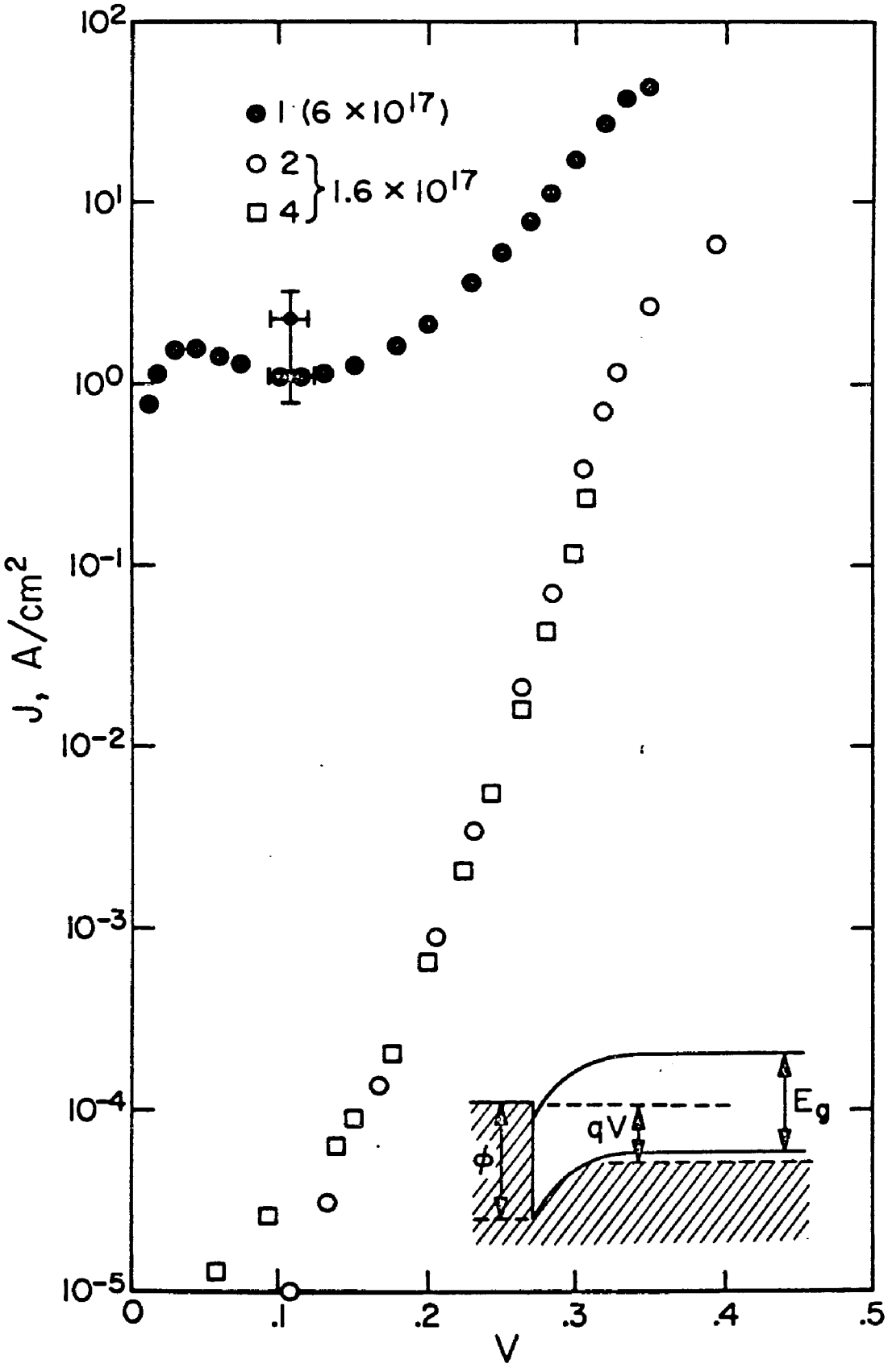

Fig. 15. Typical 77° K current-voltage plots for Schottky barriers on p-type InAs.

before the current level rises to the point where resistive drop becomes important. Since the InAs surface is highly n-type,[24] the effects of surface leakage at low current levels are more severe than with GaAs. This effect and room-temperature blackbody radiation made the data unusable below approximately 10^{-4} A/cm^2 even in the better samples.

The dependence of the imaginary part of the wave vector k on energy E was determined from the measured current I at applied forward voltage V by Eq. 10. Results of this procedure are shown in Fig. 16.

On samples 2-5, the barrier energy ϕ_B and carrier concentration N were determined from 77° K capacitance vs. reverse bias voltage using a dielectric constant ε of 12.6.

On sample 1 the barrier energy was taken to be the voltage at the current minimum plus the band gap [24] (0.43 eV at 77° K).[27] Since the low impedance of this sample precluded measurements of capacitance vs. voltage, the carrier concentration was adjusted to bring the k values into agreement with those of the other samples in the region of overlap. This procedure gave a concentration of 6×10^{17} cm^{-3}, in good agreement with Hall measurements supplied by the manufacturer (given as 7×10^{17} cm^{-3}).

The solid curve in Fig. 16 is Franz's symmetrical two-band expression given by Eq. 4 assuming an effective mass m^* of 0.02 times the mass of the free electron. The reported values for the conduction and valence band are 0.02 and 0.025, respectively.[21]

We have also compared the magnitude of the currents with those predicted by Eq. 6 for the case of degenerate semiconductors. As shown

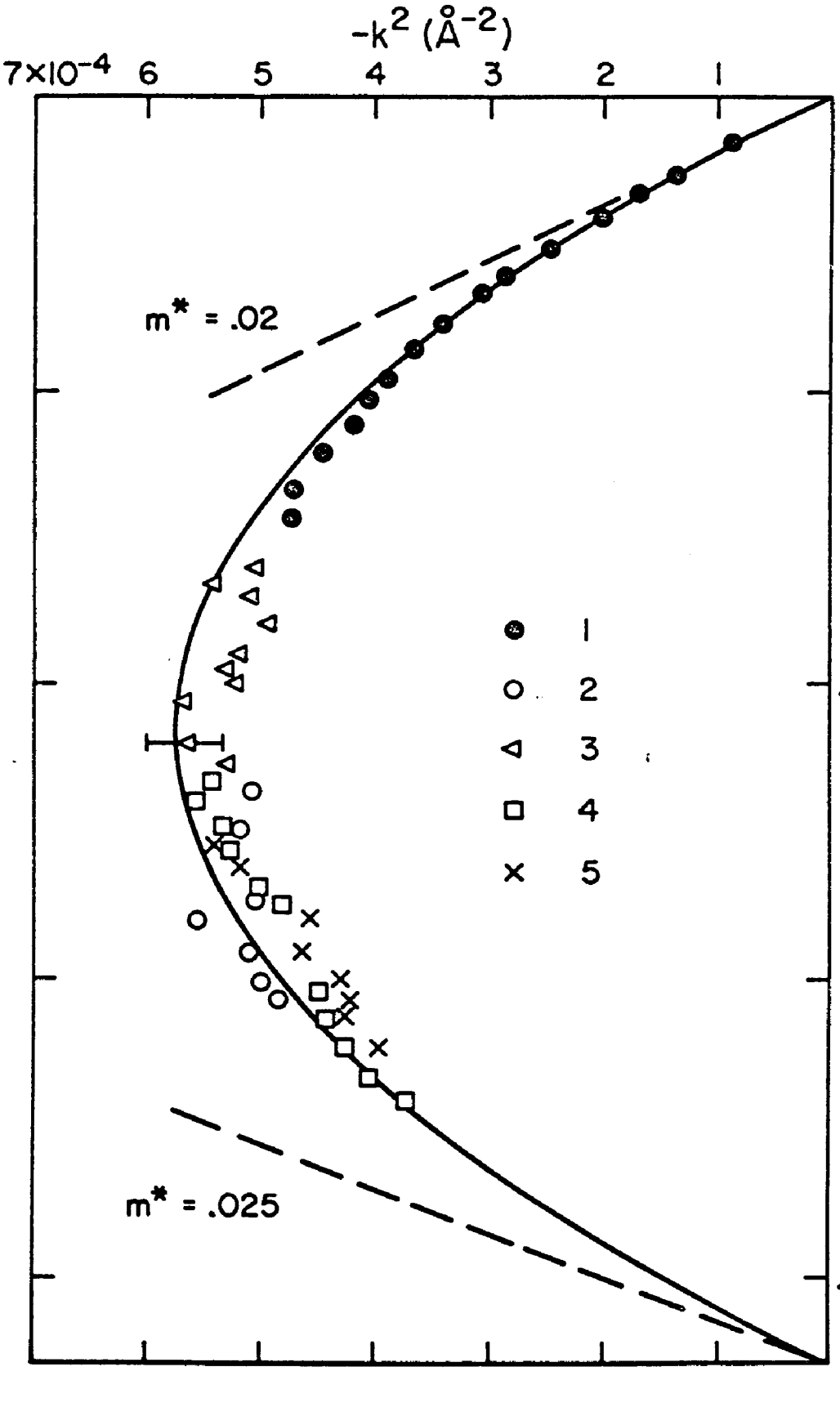

Fig. 16. Energy-wave-vector plot derived from current voltage data. The solid curve is the two-band expression for $m^* = 0.02$.

in Fig. 15 at the current minimum, sample 1 is in excellent agreement with theoretical prediction. Since the tunneling path comprises the entire forbidden gap at the minimum, the theoretical values for both an effective mass of 0.02 and 0.025 are presented. The magnitude of the current in samples 2 and 3 using the data of Table II was, however, over an order of magnitude lower than that calculated. Such a discrepancy could be accounted for by a 0.04 eV error in barrier energy. The measured value of 0.38 was determined by capacitance-voltage techniques and because of its low energy could not be verified by photoresponse measurements. As indicated earlier the variations in barrier energy do not change the slope of the forward log J-V characteristics. However, a higher barrier energy would have the effect of shifting the theoretical J-V characteristics into agreement with those observed and shifting the corresponding points in Fig. 16 downward more in agreement with the 0.025 effective mass at the valence band.

Chapter V

Conclusion

The experimental results presented for CdTe are in excellent agreement with theoretical predictions for electron tunneling currents through the region of the forbidden gap near the conduction band edge. The reverse characteristics indicated a departure from the parabolic model near midgap and, in fact, presented strong evidence for the two-band model. The magnitudes of the tunneling currents for both forward and reverse biases were also found to be in good agreement with theoretical predictions. We have shown in CdTe that trapping states can act as intermediate states to greatly increase the tunneling probability and reduce the slope of the log J-V curves by a factor of two under the proper conditions. It was also possible to calculate the energy level of the traps involved in the intermediate state case and to obtain an estimate of their density. Finally in InAs, by virtue of its unique nature, the E-k dispersion relation for nearly the entire forbidden gap was mapped out. The experimental results are in excellent agreement with the two-band model.

Thus, we have shown in this work the appropriateness of the existing theoretical models which will thereby permit the use of Schottky barrier tunneling characteristics as a powerful tool in the study of semiconductors.

References

1. C. A. Mead, Solid State Electronics 9, 1023 (1966).

2. N. F. Mott, Proc. Roy. Soc. (London) A171, 281 (1939); A171, 27 (1939).

3. W. Schottky, Z. Physik 113, 367 (1939); 118, 539 (1942).

4. H. A. Bethe, MIT Radiation Laboratory Report, No. 43/12 (1942) unpublished.

5. G. W. Lewicki, Thesis, California Institute of Technology, 1965 (unpublished).

6. G. W Lewicki and C. A. Mead, Phys. Rev. Letters 16, 939 (1966).

7. R. Stratton, G. W. Lewicki and C. A. Mead, Solid State Electronics 27, 1599 (1966).

8. F. A. Padovani and R. Stratton, Phys. Rev. Letters 16, 1202 (1966).

9. J. W. Conley and G. D. Mahan, Phys. Rev. 161, 681 (1967).

10. M. F. Millea, M. McColl and C. A. Mead, Phys. Rev. 177, 1164 (1969).

11. F. A. Padovani and R. Stratton, Solid State Electronics 9, 695 (1966).

12. W. Franz, Handbuch der Physik (Verlag-Springer, Berlin, 1956), edited by S. Flugge, Vol. XVII.

13. G. H. Parker and C. A. Mead, Phys. Rev. Letters 21, 605 (1968).

14. J. W. Conley and G. D. Mahan, Phys. Rev. 161, 681 (1967).

15. C. R. Crowell, Solid State Electronics 8, 395 (1965).

16. J. McDougall and E. C. Stoner, Roy. Soc., London, Trans. 237A, (1938).

17. G. H. Parker and C. A. Mead, Appl. Phys. Letters 14, 21 (1969).

18. A. S. Grove, Physics and Technology of Semiconductor Devices (J. Wiley & Sons, Inc., New York, 1967).

19. W. Shockley and W. T. Read, Phys. Rev. 87, 835 (1952).

20. R. N. Hall, Phys. Rev. 87, 387 (1952).

21. Benoit à la Guillaume, "Constantes Selectionees Relatives aux Semiconducteurs," (Pergamon Press, S. A. R. L., Paris, 1961).

22. E. L. Murphy and R. H. Good, Jr., Phys. Rev. 102, 1464 (1956).

23. M. M. Atalla and R. W. Soshea, Scientific Report No. 1, 1962, Contract Nr AF 19(628)-1637 hpa.

24. F. Padovani, in "Physics of III-V Compounds," (Academic Press, Inc., New York, to be published).

25. F. T. J. Smith, "Electrically Active Point Defects in CdTe," Trans. Metallurgical Soc. AIME, in press.

26. C. A. Mead and W. G. Spitzer, Phys. Rev. Letters 10, 471 (1963).

27. E. O. Kane, private communication.